



An adaptive method for computing resonance fields for continuous-wave EPR spectra

Stefan Stoll, Arthur Schweiger *

Physical Chemistry Laboratory, ETH Hönggerberg, CH-8093 Zürich, Switzerland

Received 17 July 2003; in final form 4 September 2003

Published online: 7 October 2003

Abstract

We present an efficient method for computing resonance fields for cw EPR that adaptively models the state energies over a given field range with cubic splines. The method diagonalizes the spin Hamiltonian matrix for suitably chosen fields, which are determined by an adaptive iterative bisection procedure. Resonance fields are computed from the cubic spline model. The new method adapts to the complexity of the spin system and keeps the number of diagonalizations minimal. For systems with field-independent interactions (FII) small compared to the spectrometer frequency ν_0 only three diagonalizations are needed, for high-spin systems with FII larger than ν_0 up to 60 diagonalizations are necessary.

© 2003 Elsevier B.V. All rights reserved.

1. Introduction

The extraction of spin Hamiltonian (sH) parameters from the positions of resonances is the essential part in the analysis of continuous-wave (cw) EPR spectra. For that purpose, resonance fields or full spectra are computed for different sets of sH parameters and compared to the experimental data.

There exist two different approaches to compute resonance fields. One uses approximate analytical formulas derived mainly by means of perturbation

theory. Although important for gaining physical insight, such formulas are less useful for general spectral simulations, since their validity is often severely restricted. They have been entirely superseded by schemes that use fully numerical methods. These methods construct a matrix representation \mathcal{H} of the sH and compute the states and state energies from its eigenvalues E_u and eigenvectors $|u\rangle$ using standard numerical diagonalization algorithms. Resonance fields and transition intensities are then determined from E_u and $|u\rangle$.

There are several methods described in the literature for computing resonance fields based on matrix diagonalization. However, they are not generally applicable and rely on certain assumptions about the spin system. In this Letter we introduce a method which is based on an adaptive

* Corresponding author. Fax: +41-1-6321021.

E-mail address: schweiger@phys.chem.ethz.ch (A. Schweiger).

segmentation procedure [1]. It is general, robust and quick.

In the next section we present the relevant equations for computing the resonance fields and their direct numerical solution by the eigenfield approach. Then we classify and discuss known approximate methods and their problems. This is followed by a presentation of the new adaptive iterative bisection method. Finally, characteristics and advantages of the new scheme are discussed.

2. Resonance fields

Suppose we have a spin system consisting of an arbitrary number of coupled electron and nuclear spins with a total of N spin states. For our purpose it is sufficient to use the sH \mathcal{H} in the general form

$$\mathcal{H}(\mathbf{B}) = \mathcal{F} + B \mathcal{G}(\mathbf{n}), \quad (1)$$

with the magnitude $B = |\mathbf{B}|$ of the external magnetic field. All field-independent interactions are collected in matrix \mathcal{F} , all Zeeman interactions are contained in matrix \mathcal{G} , which depends on the orientation $\mathbf{n} = \mathbf{B}/B$ of the magnetic field with respect to a molecule-fixed frame. The spin system and its interactions can be of any complexity as long as the sH has the above general form. In the following, we always use frequency units, i.e. $H = \mathcal{H}/\hbar$, $F = \mathcal{F}/\hbar$, etc.

The eigenstates $|u\rangle$ of the spin system satisfy the Schrödinger equation

$$H(\mathbf{B})|u\rangle = E_u|u\rangle, \quad (2)$$

where E_u is the energy of state $|u\rangle$. Both E_u and $|u\rangle$ depend on \mathbf{B} . States are numbered from 1 to N from lowest to highest energy. For certain values of \mathbf{B} , two or more states can be degenerate. Since these degeneracies occur only at a finite number of isolated points in \mathbf{B} space [2], $v > u$ implies $E_v \geq E_u$ for all \mathbf{B} , and the state ordering is unique and unambiguous.

In a field-swept cw EPR experiment the magnetic field B is varied, and resonance between states $|u\rangle$ and $|v\rangle$ occurs if B is such that the difference $\Delta_{uv}(B) = E_v(B) - E_u(B)$ matches the spectrometer frequency ν_0 , or, in other words, if the resonance function $R_{uv}(B)$ becomes zero

$$R_{uv}(B) = E_v(B) - E_u(B) - \nu_0 = 0. \quad (3)$$

This corresponds to two eigensystem equations coupled by E_u and B

$$\begin{aligned} (F + BG)|u\rangle &= E_u|u\rangle, \\ (F + BG)|v\rangle &= (E_u + \nu_0)|v\rangle, \end{aligned} \quad (4)$$

where we have abbreviated $G(\mathbf{n})$ by G .

If the overall splitting at $B = 0$ is not larger than the spectrometer frequency, i.e. if $\Delta_{1N}(0) = E_N(0) - E_1(0) \leq \nu_0$, only one resonance field B_{uv} per state pair ($|u\rangle, |v\rangle$) can occur. For $\Delta_{1N}(0) > \nu_0$, an arbitrary number of resonance fields (some of them occur in pairs and are the so-called looping resonance fields) is possible.

Eqs. (4) can be combined and transformed to the N^2 -dimensional Liouville space [3]. The resulting eigenfield equation

$$(\nu_0 \mathbf{I} \otimes \mathbf{I} - F \otimes \mathbf{I} + \mathbf{I} \otimes F^*)Z = B(G \otimes \mathbf{I} - \mathbf{I} \otimes G^*)Z \quad (5)$$

can be solved directly and gives the resonance fields (eigenfields) B_{uv} for the transitions (eigenvectors) $Z_{uv} = |u\rangle \otimes |v\rangle$. At B_{uv} , states $|u\rangle$ and $|v\rangle$ are at resonance. \otimes is the Kronecker tensor product, and \mathbf{I} denotes the state-space identity matrix.

The numerical solution of Eq. (5) is computationally very expensive, since matrices with N^4 elements are involved. The method is feasible only for small spin systems and is too slow for general use.

3. State-space methods

Approximate methods in N -dimensional state space are much faster than the eigenfield method in N^2 -dimensional Liouville space, but they are either limited in scope or need user configuration. Methods are known since more than twenty years and fall into three categories: extrapolation, interpolation and root searching.

Extrapolation methods [4–10] diagonalize the sH at one field value B_0 and use derivatives of E_u and E_v with respect to B to extrapolate linearly or quadratically to $\Delta_{uv}(B) = \nu_0$. All methods employing Taylor series or perturbational expansions belong to this class. They are only valid in a small region around B_0 .

Interpolation methods [11–13] diagonalize the sH at two field values B_q and B_r and obtain the point $A_{uv}(B) = v_0$ by linear or cubic interpolation in between. Chebyshev interpolation has been used, too. These methods are valid only between B_q and B_r and work only if $\Delta B_{qr} = B_r - B_q$ is small.

The third group uses standard root search algorithms for each transition to obtain the resonance fields. Most common is the linear Newton–Raphson method [14–20], but a more efficient quadratic method [21,22] and a least-squares approach [23] have been used as well. Root-searching methods can only find one resonance field per transition and are limited to narrow regions where $E_u(B)$ is well-behaved.

All three classes of methods work only over a small field range. If larger ranges are searched for resonances, they are usually subdivided into a fixed number of segments, with either constant [10] or geometrically increasing [11] segment length. A recursive iterative bisection has also been used [20]. The segments are then separately searched for resonances. This segmentation is especially important in the case of looping transitions, since all algorithms can locate only one resonance per segment. The drawback of fixed segmentation procedures is that the number of segments is never optimal, since it has to be given by the user in advance.

For numerical diagonalization of a sH matrix, the QL algorithm [24] is generally used. Inverse iteration [24] has been used to diagonalize a sH matrix starting from the known solution of a similar matrix [19].

4. The new method

The method presented in this work proceeds in two steps. First, an accurate polynomial model of the state energies $E_u(B)$ over the magnetic field range of interest is obtained by computing state energies for selected magnetic fields (knots) and constructing interpolating cubic polynomials (splines) between them. The knots are obtained by iterative bisection starting from the initial segment $[B_{\min}, B_{\max}]$. Field segments are divided by placing a new knot at the center until all segments are either accurately modelled or do not contain reso-

nance fields. Second, the resulting cubic spline model is used to compute the resonance fields by standard root finding algorithms. The corresponding resonant states are obtained by linear interpolation.

4.1. Cubic spline model

At the outset, the two sH matrices F and G , the field range limits B_{\min} and B_{\max} (with $0 \leq B_{\min} < B_{\max}$), and the spectrometer frequency v_0 are given.

For any magnetic field value B_q , E_u and $|u\rangle$ are obtained by numerically diagonalizing the matrix $H = F + B_q G$ using the QL method [24]. The derivatives $E'_u = \partial E_u / \partial B$ at this knot are obtained from the Hellmann–Feynman theorem [16]

$$E'_u = \langle u | H' | u \rangle = \langle u | G | u \rangle. \quad (6)$$

Once the resonance fields are found, these derivatives will also be needed for the computation of transition intensities $\gamma_{uv} |\langle u | G(\mathbf{n}_1) | v \rangle|^2$ (with the direction \mathbf{n}_1 of the excitation field \mathbf{B}_1), since they appear in the expression for the generalized $1/g$ factor [16] $\gamma_{uv} = (\partial A_{uv} / \partial B)^{-1} = (E'_v - E'_u)^{-1}$.

Between two knots B_q and B_r , $E_u(B)$ can now be approximated by a cubic polynomial

$$\tilde{E}_u(B) = \mathbf{t}^T M \mathbf{e}_u = (t^3 \quad t^2 \quad t \quad 1) M \begin{pmatrix} E_u(B_q) \\ E_u(B_r) \\ \Delta B_{qr} E'_u(B_q) \\ \Delta B_{qr} E'_u(B_r) \end{pmatrix}, \quad (7)$$

with $t = (B - B_q) / \Delta B_{qr}$, $\Delta B_{qr} = B_r - B_q$, and

$$M = \begin{pmatrix} 2 & -2 & 1 & 1 \\ -3 & 3 & -2 & -1 \\ 0 & 0 & 1 & 0 \\ 1 & 0 & 0 & 0 \end{pmatrix}. \quad (8)$$

This so-called Hermite cubic spline polynomial $\tilde{E}_u(B)$ passes through the two segment border points $E_u(B_q)$ and $E_u(B_r)$ with the two slopes $E'_u(B_q)$ and $E'_u(B_r)$, respectively.

Between the border points, this polynomial will deviate to some degree from the true $E_u(B)$ curve, as illustrated in Fig. 1. It is not possible to determine the maximum deviation δ_u without evaluating the entire $E_u(B)$ dependence. Instead, an

estimate of this deviation can be obtained by comparing \tilde{E}_u at the segment center $B_s = (B_q + B_r)/2$ (i.e. $t = 1/2$)

$$\tilde{E}_u(B_s) = \frac{1}{2}[E_u(B_q) + E_u(B_r)] + \frac{\Delta B_{qr}}{8} \times [E'_u(B_q) - E'_u(B_r)] \quad (9)$$

to the correct energy $E_u(B_s)$. The center deviation

$$\epsilon_u = |E_u(B_s) - \tilde{E}_u(B_s)| \quad (10)$$

is then an estimate of the modelling error of the spline for state energy E_u (see Fig. 1). An estimate for the overall error for a transition frequency is

$$\epsilon = 2 \max_u \epsilon_u. \quad (11)$$

The iterative bisection is terminated under two conditions. First, a segment is not divided, if the modelling error of Eq. (11) is below a given threshold

$$\epsilon < \epsilon_0. \quad (12)$$

Resonance fields are sufficiently accurate for spectral simulations if ϵ_0 is set to $10^{-3}v_0$. Alternatively, an absolute threshold (e.g. $\epsilon_0 = 0.1$ MHz) can be used.

Second, a segment $[B_q, B_r]$ also does not have to be further subdivided if it does not contain any resonances $\Delta_{uv}(B) = v_0$ for any state pair ($|u\rangle, |v\rangle$). Two simple tests can be used to establish the absence of resonances even before the exact depen-

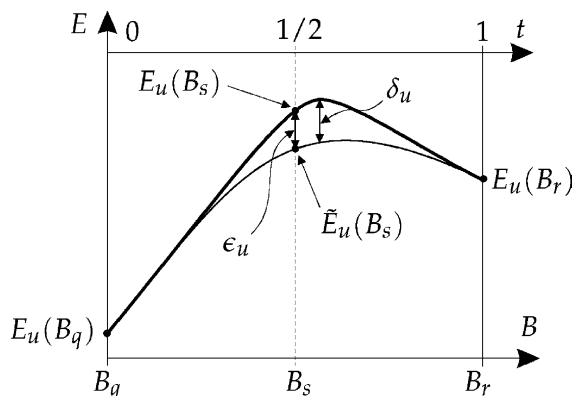


Fig. 1. Approximation of a state energy E_u as a function of the magnetic field B by a cubic spline $\tilde{E}_u(B)$. δ_u and ϵ_u are the maximum and the center deviation, respectively.

dence of $\Delta_{uv}(B)$ is known. First, a segment with $\Delta_{1N}(B_r) < v_0$ does not contain resonances, since $\Delta_{1N}(B)$ increases monotonically with B [3]. The second test depends on $\Delta_{1N}(0)$. If $\Delta_{1N}(0) \leq v_0$, there is only one resonance per state pair, and the resonance function R_{uv} changes sign

$$R_{uv}(B_q)R_{uv}(B_r) \leq 0 \quad (13)$$

if there is a resonance in the segment $[B_q, B_r]$. If all state pairs fail this test, the segment is not bisected further.

On the other hand, if $\Delta_{1N}(0) > v_0$, more than one resonance can occur, and the test is more complex. For the usual spin Hamiltonian of the form given in Eq. (1), the maximum derivative of a state energy is

$$\lambda = \max_{u,B} E'_u(B) = E'_N(\infty) = \frac{\mu_B}{h} \sum_k |\mathbf{n}^T \mathbf{g}^{(k)}| S^{(k)} + \frac{\mu_n}{h} \sum_l g_n^{(l)} I^{(l)}. \quad (14)$$

($S^{(k)}$ and $I^{(l)}$ are the primary spin quantum numbers of the spins in the system.) As a consequence, the maximum and the minimum possible derivatives of a transition function Δ_{uv} are 2λ and -2λ , respectively. Any transition function will therefore lie in the bounding parallelogram shown in Fig. 2. If the horizontal line $\Delta_{uv}(B) = v_0$ does not pass through the parallelogram, i.e. if

$$\left| \frac{\Delta_{uv}(B_q) + \Delta_{uv}(B_r)}{2} - v_0 \right| > \lambda \Delta B, \quad (15)$$

there are no resonances between states $|u\rangle$ and $|v\rangle$ in the segment. Otherwise, resonances cannot be excluded as long as the exact dependence $\Delta_{uv}(B)$ is not known.

In summary, the above adaptive segmentation algorithm proceeds as follows.

```

diagonalize  $H$  at  $B_{\min}$  and  $B_{\max}$ 
knots = ( $B_{\min}$   $B_{\max}$ )
finished(1) = false
repeat
  s = an unfinished segment [ $B_s$   $B_{s+1}$ ]
  if  $\Delta_{1N}(B_{s+1}) > v_0$ 
    if  $\Delta_{1N}(0) < v_0$ 
      ResonPossible = test Eq. (13)
    else

```

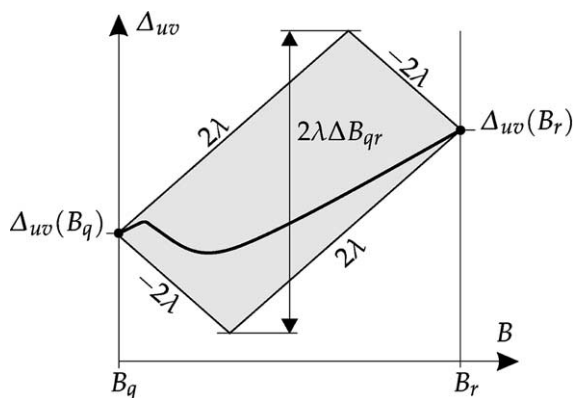


Fig. 2. Bounding region (shaded) for the transition energy Δ_{uv} between states $|u\rangle$ and $|v\rangle$ as a function of the magnetic field B over a segment $[B_q, B_r]$. $\Delta B_{qr} = B_r - B_q$, and λ is the maximum energy derivative $E'_N(\infty)$.

```

ResonPossible = test Eq. (15)
else ResonPossible = false
if ResonPossible
     $B_{\text{new}} = (B_s + B_{s+1})/2$ 
    diagonalize  $H$  at  $B_{\text{new}}$ 
    compute  $\epsilon$  at  $B_{\text{new}}$  (Eq. (11))
    insert  $B_{\text{new}}$  as new knot between  $B_s$  and  $B_{s+1}$ 
    finished(s) = finished(s+1) =  $\epsilon \leq \epsilon_0$ 
else finished = true
until all finished

```

Note that the error of a segment is only computed if resonances cannot be excluded.

4.2. Locating resonance fields

After modelling the dependence of the state energies over the range $[B_{\min}, B_{\max}]$, the second step of the new method locates the resonance fields at the spectrometer frequency ν_0 for all transitions. For a given state pair $(|u\rangle, |v\rangle)$ and a given segment, the roots t_{uv} of the resonance polynomials

$$\tilde{R}_{uv}(t) = \tilde{\Delta}_{uv} - \nu_0 = \mathbf{t}^T \mathbf{p} - \nu_0 \quad (16)$$

with $\mathbf{p} = (p_3, p_2, p_1, p_0)^T = M(\mathbf{e}_v - \mathbf{e}_u)$ give the resonance fields $B_{uv} = B_q + t_{uv}\Delta B_{qr}$. If looping resonances cannot occur, i.e. when $R_{1N}(0) > 0$, at most one root is possible for each transition, and \tilde{R}_{uv} changes sign in the segment where the resonance is located (see Eq. (13)). In this case the Newton–Raphson method with

$$t_0 = -\frac{\Delta_{uv}(B_q)}{\Delta_{uv}(B_r) - \Delta_{uv}(B_q)}, \quad (17)$$

$$t_{n+1} = t_n - \frac{p_3 t_n^3 + p_2 t_n^2 + p_1 t_n + p_0 - \nu_0}{3p_3 t_n^2 + 2p_2 t_n + p_1}$$

is fastest to locate the root. If looping resonances are possible, the discriminant $d = p_2^2 - 3p_3p_1$ is computed. For $d \leq 0$, the polynomial is monotonic, has only one distinct root, and the above root-finding iteration can be used. In the case of $d > 0$, up to three resonances are possible. They can be obtained from analytical expressions [24]. The cubic polynomials have to be tested for roots only in segments which do not satisfy the resonance exclusion criterion Eq. (15).

When a resonance B_{uv} is found, the resonant state vectors $|u\rangle$ and $|v\rangle$ can be computed by linear interpolation between the two adjacent knots using

$$|u\rangle(B_{uv}) = \frac{B_r - B_{uv}}{\Delta B_{qr}} |u\rangle(B_q) + \frac{B_{uv} - B_q}{\Delta B_{qr}} |u\rangle(B_r) \quad (18)$$

with a similar expression for $|v\rangle$. It is crucial to align the phases of the state vectors $|u\rangle(B_q)$ and $|u\rangle(B_r)$ before the interpolation, e.g. by rotating them so that the largest elements of both vectors are real and positive. Cubic interpolation is not necessary, since Eq. (18) is sufficiently accurate in all cases.

5. Discussion

In terms of the classification used in Section 2, the new method is a cubic interpolation approach with adaptive segmentation. Its main characteristic is that the number of segments and hence the number of time-consuming diagonalizations is automatically adapted to the complexity of the field dependence of the state energies. Apart from the physical and experimental parameters F , G , B_{\min} , B_{\max} and ν_0 , no user parameters are required.

The performance of the new method can be measured by the number of diagonalizations per resonance field and by comparing the accuracy of the resonance fields computed with this approach with the exact ones from the eigenfield equation Eq. (5). Both measures depend on the relation between $\Delta_{1N}(0)$ and ν_0 .

For systems with $S = 1/2$ in high-field situations with $\Delta_{1N}(0) < \nu_0/4$, the new method needs two segments and consequently only three diagonalizations, independent of the total number of states N or the number of resonances. With $\epsilon_0 = 10^{-3}\nu_0$, we have found that the maximum relative error in the resonance fields is always $< 10^{-5}$.

Low- and intermediate-field situations with $S > 1/2$, where $\Delta_{1N}(0) > \nu_0/4$, are more complex. A typical example is illustrated in Fig. 3. The adaptive segmentation procedure increases the segment density in the vicinity of anticrossings, since sharp turns are the most difficult to model with smooth cubic splines. If an anticrossing is off-resonant (e.g. at 575 mT), it is not accurately modelled. In the worst case, around 10 diagonalizations per resonance field are needed, but the value is usually much lower. The error of the resonance fields is commonly below $10^{-4}(B_{\max} - B_{\min})$. Compared to a linear segmentation with the same number of segments, the new method gives resonance fields which are 10–100 times more accurate on average.

For the simulation of powder spectra the new method has the advantage that it adapts to the complexity of the $E_u(B)$ dependence when the orientation \mathbf{n} of the magnetic field changes. If \mathbf{n} is close to a principal axis of an interaction tensor or

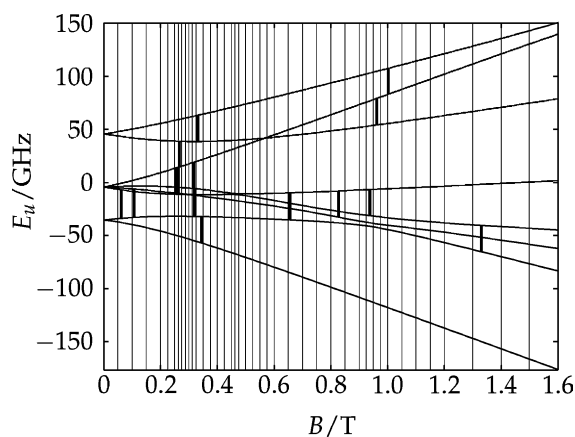


Fig. 3. Segmentation and resonance fields as obtained by the adaptive iterative bisection for Tb^{4+} in a ThO_2 single crystal [25]. sH parameters: $S = 7/2$, $g = 2.0146$, $60B_4 = -2.528$ GHz, $1260B_6 = -24.84$ MHz, $\mathbf{n}^T = (0.0493, 0.0493, 0.9976)$. $\nu_0 = 25$ GHz, $B_{\min} = 0$ T, $B_{\max} = 1.6$ T, threshold $\epsilon_0 = 25$ MHz. Forty three segments, 15 resonance fields, maximum resonance field error $4.5\mu\text{T}$.

matrix of the sH, the anticrossings are sharper, and a number of segments larger than for non-canonical orientations is needed. For the system in Fig. 3, 43 segments are required along principal axes, whereas as few as 16 segments are needed for the other orientations. The savings in terms of number of diagonalizations are significant: The average number of segments per orientation is 22.7 (for a total of 496 orientations over one octant). A non-adaptive segmentation would have to take 43 segments for all orientations.

Another advantage of the adaptive cubic spline model is that it allows for an accurate computation of asymmetric line shapes as they occur near coalescence points of looping transitions [13]. In addition, resonance fields for several spectrometer frequencies ν_0 can be computed from the same cubic spline model. This accelerates multi-spectral fittings.

Although the algorithm presented above is straightforward, there seems to be little place for improvement. Instead of cubic splines, higher-order polynomials could be used. We have examined the performance of quintic splines where, at each knot, $|u|'$ and E_u'' have to be evaluated [1] in addition to E_u' . In general they need 10–30% fewer knots than cubic splines to achieve the same overall modelling error, but the inconvenience of having to compute $|u|'$ and E_u'' at each knot outweighs the savings in the number of knots.

The method presented in this Letter is applicable to isotropic and anisotropic spin systems for both cw EPR and cw NMR. Although it was designed for spin Hamiltonians of the form given in Eq. (1), it can be adapted to include terms of higher order in magnetic field B by using $E_N'(B_{\max})$ instead of $E_N'(\infty)$ in Eq. (14).

The adaptive segmentation algorithm has been implemented in the program package EasySpin [1] for use with the scientific software MATLAB (The Mathworks, Inc, Natick, MA, USA). It is available from <http://www.esr.ethz.ch>.

Acknowledgements

This project was supported by the Swiss National Science Foundation. We thank Høgni

Weihe (University of Copenhagen), Chris Noble (University of Queensland), and Betty Gaffney (Florida State University) for providing details about their resonance field computation algorithms.

References

- [1] S. Stoll, Ph.D. thesis, ETH Zürich, 2003.
- [2] T. Kato, *A Short Introduction to Perturbation Theory for Linear Operators*, Springer, New York, 1982.
- [3] G.G. Belford, R.L. Belford, J.F. Burkhalter, *J. Magn. Reson.* 11 (1973) 251.
- [4] R.L. Belford, P.H. Davies, G.G. Belford, T.M. Lenhardt, *Am. Chem. Soc. Symp. Ser.* 5 (1974) 40.
- [5] M. Nilges, Ph.D. thesis, University of Illinois, Urbana, 1979.
- [6] M.I. Scullane, L.K. White, N.D. Chasteen, *J. Magn. Reson.* 47 (1982) 383.
- [7] C.P. Keijzers, R.J. Reijerse, P. Stam, M.F. Dumont, M.C.M. Gribnau, *J. Chem. Soc. Faraday Trans.* 183 (1987) 3493.
- [8] M.C.M. Gribnau, J.L.C. van Tits, E.J. Reijerse, *J. Magn. Reson.* 90 (1990) 474.
- [9] D. Wang, G.H. Hanson, *Appl. Magn. Reson.* 11 (1996) 401.
- [10] M. Griffin, A. Muys, C. Noble, D. Wang, C. Eldershaw, K.E. Gates, K. Burrage, G.R. Hanson, *Mol. Phys. Rep.* 26 (1999) 60.
- [11] J. Glerup, H. Weihe, *Acta Chem. Scand.* 45 (1991) 444.
- [12] F.E. Mabbs, D. Collison, *Electron Paramagnetic Resonance of d Transition Metal Compounds*, Elsevier, Amsterdam, 1992.
- [13] B.J. Gaffney, H.J. Silverstone, *J. Magn. Reson.* 134 (1998) 57.
- [14] J.D. Swalen, H.M. Gladney, *IBM J. Res. Dev.* 8 (1964) 515.
- [15] H. Rinneber, J.A. Weil, *J. Chem. Phys.* 56 (1972) 2019.
- [16] G. van Veen, *J. Magn. Reson.* 30 (1978) 91.
- [17] A. Kreiter, J. Hüttermann, *J. Magn. Reson.* 93 (1991) 12.
- [18] B. Gaffney, H.J. Silverstone, *Biol. Magn. Reson.* 13 (1993) 1.
- [19] K.E. Gates, M. Griffin, G.H. Hanson, K. Burrage, *J. Magn. Reson.* 135 (1998) 103.
- [20] G. Morin, D. Bonnin, *J. Magn. Reson.* 136 (1999) 176.
- [21] J.H. Mackey, M. Kopp, E.C. Tynan, T.F. Yen, in: T.F. Yen (Ed.), *Electron Spin Resonance of Metal Complexes*, Plenum Press, New York, 1969, p. 33.
- [22] D. Nettar, J.J. Villafranca, *J. Magn. Reson.* 64 (1985) 61.
- [23] S.K. Misra, *J. Magn. Reson.* 140 (1999) 179.
- [24] W.H. Press, S.A. Teukolsky, W.T. Vetterling, B.P. Flannery, *Numerical Recipes in C*, Cambridge University Press, Cambridge, 1992.
- [25] J.M. Baker, J.R. Chadwick, G. Garton, J.P. Hurrell, *Proc. Roy. Soc. London A* 286 (1965) 352.